PAPER • **OPEN ACCESS**

Ultra-broadband absorbance of nanometer-thin pyrolyzed-carbon film on silicon nitride membrane

To cite this article: Justinas Jorudas *et al* 2024 *Nanotechnology* **35** 305705

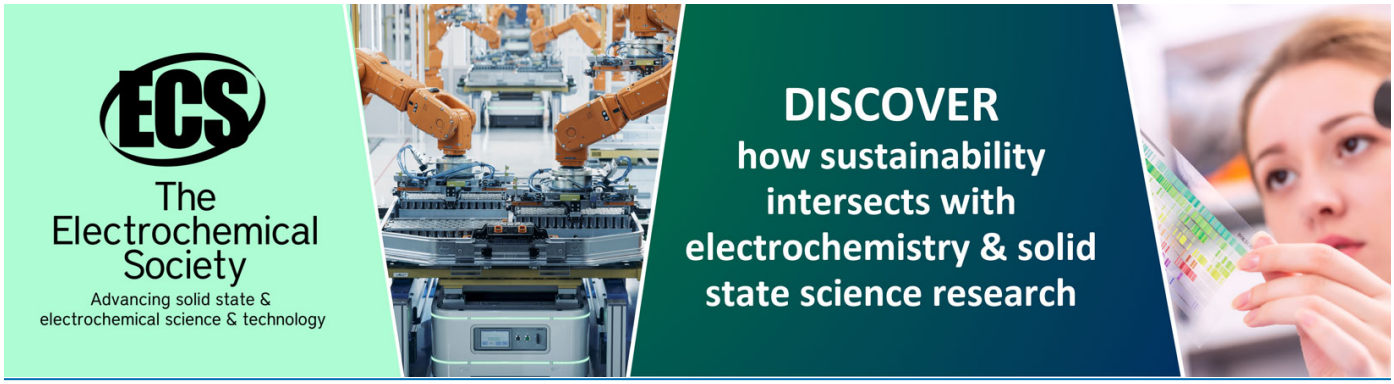

OPEN ACCESS
IOP Publishing
Nanotechnology

Nanotechnology **35** (2024) 305705 (7pp)
https://doi.org/10.1088/1361-6528/ad4157

Ultra-broadband absorbance of nanometer-thin pyrolyzed-carbon film on silicon nitride membrane

Justinas Jorudas[1,2,7], Hamza Rehman[1,7], Maria Cojocari[1], Daniil Pashnev[2], Andrzej Urbanowicz[2,3], Irmantas Kašalynas[2,4], Benedetta Bertoni[5], Leonardo Vicarelli[5], Alessandro Pitanti[5,6], Sergei Malykhin[1], Yuri Svirko[1], Polina Kuzhir[1] and Georgy Fedorov[1,*]

[1] Department of Physics and Mathematics, Center of Photonics Research, University of Eastern Finland, Yliopistokatu 7, FI-80101 Joensuu, Finland
[2] Department of Optoelectronics, Center for Physical Sciences and Technology (FTMC), Saulėtekio av. 3, LT-10257 Vilnius, Lithuania
[3] UAB 'TERAVIL', Savanoriu av. 235, LT-02300, Vilnius, Lithuania
[4] Institute of Applied Electrodynamics and Telecommunications, Vilnius University, Saulėtekio al. 3, 10257 Vilnius, Lithuania
[5] Dipartimento di Fisica, Università di Pisa, largo Bruno Pontecorvo 3, I-56127 Pisa, Italy
[6] NEST, CNR—Istituto Nanoscienze, piazza San Silvestro 12, I-56127 Pisa, Italy

E-mail: alessandro.pitanti@unipi.it and georgy.fedorov@uef.fi

Received 30 November 2023, revised 13 March 2024
Accepted for publication 22 April 2024
Published 9 May 2024

Abstract

Fifty percents absorption by thin film, with thickness is much smaller than the skin depth and optical thickness much smaller than the wavelength, is a well-known concept of classical electrodynamics. This is a valuable feature that has been numerously widely explored for metal films, while chemically inert nanomembranes are a real fabrication challenge. Here we report the 20 nm thin pyrolyzed carbon film (PyC) placed on 300 nm thick silicon nitride (Si_3N_4) membrane demonstrating an efficient broadband absorption in the terahertz and near infrared ranges. While the bare Si_3N_4 membrane is completely transparent in the THz range, the 20 nm thick PyC layer increases the absorption of the PyC coated Si_3N_4 membrane to 40%. The reflection and transmission spectra in the near infrared region reveal that the PyC film absorption persists to a level of at least 10% of the incident power. Such a broadband absorption of the PyC film opens new pathways toward broadband bolometric radiation detectors.

Keywords: ultra-broadband absorption, thin-film absorber, pyrolytic carbon, terahertz, near-infrared

1. Introduction

Thin absorptive coatings are widely used in microwave and THz regions as polarizers, filters, attenuators, antennas and electromagnetic interference shielding layers [1–9]. Graphene and carbon-based thin films are very attractive in this respect because their electromagnetic response can be engineered by modifying synthesis conditions [10], doping [11], biasing [12], laser irradiation [13] and mechanical deformation [14]. These also include bolometric detection of radiation in the mid-infrared (MIR) and terahertz (THz) ranges [15–17].

[7] These authors contributed equally.
[*] Author to whom any correspondence should be addressed.

Increasing performance of such bolometers in terms of both sensitivity and response time requires reduction of the footprint, that imposes restrictions on the efficiency of converting the radiation energy into heat.

It can be shown that the peak absorption of 50% can be reached when sheet resistance of film $R_{sh} = \rho/d$, where ρ is the material resistivity and d is the thickness of the film, is equal to half of the vacuum impedance $Z_0 = \sqrt{\mu_0/\varepsilon_0} = 377\,\Omega$ [18, 19], when d is much smaller than the skin depth. This allows to introduce the 'metallicity' criterion, which reads:

$$\sigma(\omega) \gg \varepsilon_0\omega, \tag{1}$$

where $\varepsilon_0 = 8.85{\cdot}10^{-12}\,\mathrm{F\,m^{-1}}$ and ω is the frequency of the incident electromagnetic wave. Metals used for electronic applications (gold, copper, aluminum, etc.) meet the 'metallicity' criterion in a wide range of frequencies. However, their conductivity is very large, so that the thickness of a film having the $0.5 \times Z_0$ sheet resistance is too small to realize in a reproducible fabrication procedure [20, 21]. In order to avoid this bottleneck there has been suggestions to use metal alloys or doped semiconductor layers compatible with the conventional complementary metal–oxide–semiconductor (CMOS) technology [22].

The conductivity of graphitic films is about two or three orders of magnitude lower than the metal ones [23] however they have not been explored yet. Moreover, advantages of graphitic films include, but are not limited to chemical robustness, low density, ability to fabricate free-standing 3D structures [24] and ability to tune the conductivity in a wide range via the growth parameters. These features make graphitic films a good choice as an absorber material to increase the microbolometer sensitivity [25].

In this work, we report the performance of the 20 nm thin pyrolyzed carbon (PyC) film deposited on a suspended 300 nm thick silicon nitride (Si_3N_4) membrane for the absorption of radiation in THz and NIR ranges. We show that the 20 nm thick PyC film absorbs between 40% and 10% of the incoming radiation intensity in the THz and NIR ranges, respectively. Our experimental results are in line with describing the PyC film conductivity based on a Drude model with a scattering frequency of about 10^{15} Hz and open opportunities for the creation of very sensitive and fast radiation detectors operating in a wide frequency range. The fabrication of the PyC covered silicon nitride membrane rely on much more technologically friendly and reproducible routines (CVD, EBL and etching) in comparison with graphene/polymer sandwiches [26] and hemi-spheres metasurface [8].

2. Method

The PyC film was grown on a double-side polished, 250 μm thick Si wafer coated with 300 nm thick layer of high stress Si_3N_4 using low pressure chemical vapor deposition (LPCVD). The high growth temperature (~800 °C) and the different thermal expansion between Si and Si_3N_4 combine to give the film a strong in-plane tensile stress at the room

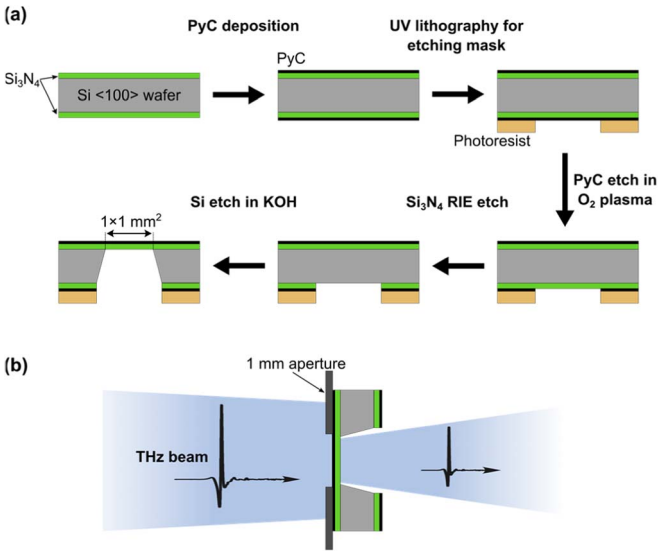

Figure 1. (a) Fabrication steps used to make the PyC-coated suspended silicon nitride membrane. (b) Schematic of PyC/Si_3N_4 membrane in transmission geometry through aperture.

temperature (~900 MPa), which is ideal for the realization of mechanical devices. The PyC film was deposited using the standard CVD process of hydrocarbon decomposition [23, 27]. A cleaned Si_3N_4/Si substrate was loaded into the CVD chamber, which was filled with hydrogen and heated to 700 °C. After that the chamber was pumped down to introduce 1:4 hydrogen-methane gas mixture at the pressure of 25 mBar, heated up to 1100 °C and kept at this temperature for 5 min and then cooled down to 700 °C. The thickness of the deposited PyC film was measured to be 20 nm, with sheet resistance of 600 $\Omega\,\mathrm{sq^{-1}}$., resulting in DC conductivity value of about $8 \times 10^4\,\mathrm{S\,m^{-1}}$. The main steps in the fabrication of the $1 \times 1\ \mathrm{mm^2}$ PyC/Si_3N_4 freestanding membrane are schematically shown in figure 1(a). After the deposition of the PyC film onto both sides of the Si_3N_4 coated Si substrate, back surface of the substrate was coated with photoresist and a $1.3 \times 1.3\ \mathrm{mm^2}$ square opening was realized by standard optical lithography and fluorine-based reaction ion etching (RIE) to remove the PyC film. Afterwards hot 30% KOH wet etching was performed to fully remove the silicon substrate. A special single-sided Teflon holder (Advanced MicroMachining Tools—GmbH) was employed during the KOH bath to protect the PyC coated side.

Transmission spectra of the PyC/Si_3N_4 in the range of 0.5–3.0 THz range were measured using a commercial THz-TDS [28] system (T-SPEC 800, TeraVil). The measurement zone was precisely controlled with the positioning PyC membrane on top of 1 mm diameter aperture, as shown in figure 1(b). THz pulse transmitted through the empty aperture was used as the reference. Unfortunately, reflection measurements from the PyC membrane were not possible to conduct due to the small area of the membrane, which is comparable with a wavelength.

PyC/Si_3N_4 was characterized using a micro-Fourier transform infrared spectroscopy (micro-FTIR) [29] spectrometer (Jasco FT-IR 6600–IRT 5200), which employs an

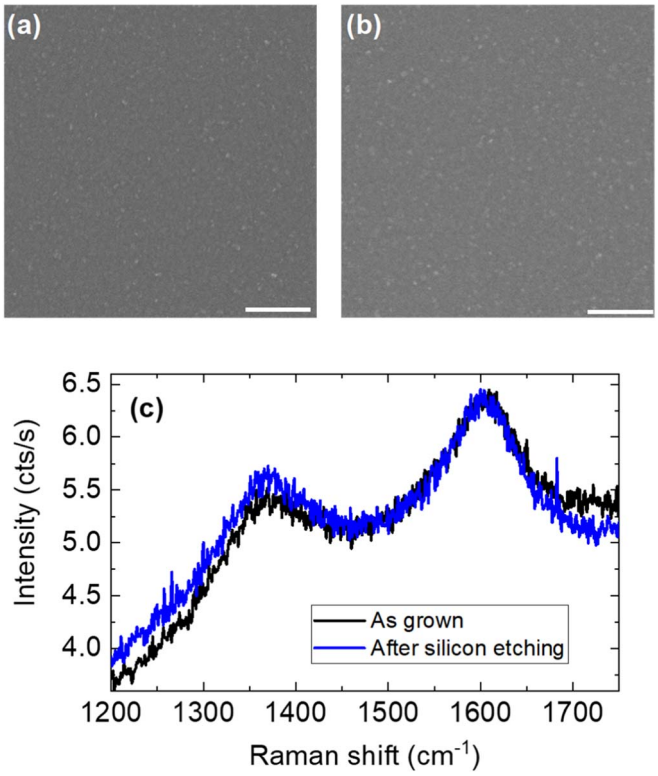

Figure 2. PyC film on silicon nitride before and after etching steps of the fabrication process. (a) SEM image of PyC as grown, (b) SEM image of PyC after Si etching process. The scale bar for both SEM images is 500 nm. (c) Raman spectra of the PyC film on silicon nitride before and after Si etching steps of the fabrication process.

interferometric setup with a movable mirror. The advantage of micro-FTIR is that the interferometer is directly mounted on a microscope head, where a broadband mid-infrared and near-infrared (MIR-NIR) source can be precisely focused with a lateral size depending on the magnification stage. In our experimental setup the final $\times 16$ objective granted for a 20 μm spot size with an aperture angle of about 35 degree. A simple modification of the optical path of the micro-FTIR can give access to both transmissivity and reflectivity measurements, enabling the direct and local estimation of absorbance.

3. Results

3.1. Material characterization: SEM and raman

In order to verify the quality of the PyC film after the fabrication steps described above, we probed its DC sheet resistance using the standard 4-probe Van-der-Pauw method, measured its Raman spectrum and investigated its morphology via scanning electron microscopy (SEM), comparing the obtained parameters with the ones investigated just after deposition. The sheet resistance was found to be 500 ± 50 Ohm sq^{-1}, having a value close to the one measured in as-grown film.

The SEM images for the as-grown PyC film (figure 2(a)) and the PyC/Si_3N_4 membrane after Si etching (figure 2(b)) show that the etching did not modify the morphology. This conclusion is also confirmed by the Raman spectra measured before and after the etching of the Si wafer, as shown in figure 2(c) by matching spectra. It is known that the PyC films fabricated by CVD process consist of few-layer graphene flakes. The relative intensity of the D-peak observed at 1350 cm^{-1} and the G-peak observed at 1600 cm^{-1} corresponds to the average flake size of about 5 nm [30].

3.2. Electromagnetic response

The transmission spectra of the bare suspended 300 nm thick Si_3N_4 membrane and one with a 20 nm thick layer of PyC film in the 0.5–3 THz range are shown in figure 3(a). Due to the dielectric nature of Si_3N_4 and small thickness, the membrane is almost completely transparent to the THz radiation, having transmission close to 1. The transmission of the PyC coated Si_3N_4 membrane is reduced to 0.500 ± 0.025 and does not change in the whole measurement range of 0.5–3.0 THz. The sharp spikes in the transmission spectra are associated with the fluctuations caused by water vapor.

Following [18], we note that transmission of a thin conductive film is monotonous function of its sheet resistance (figure 3(b)) and the value $T = 0.5$ corresponds to the sheet resistance of $\sim 500 \pm 50$ Ohm sq^{-1}, which is consistent with our results obtained by four-probe Van-der-Pauw measurements. As seen from figures 3(b), absorption of 0.4 or more is achieved in a wide range of the sheet resistance values from 75 to 420 Ohm sq^{-1}. Also, our data show that the absorption remains the same as the frequency is swept by about an order of magnitude. This implies that performance of the absorbing layer is robust and does not require precise control of the growth parameters.

We now address the question of up to what frequency range the PyC film can be used as an absorber of radiation. The condition (1) is met up to the frequency of 10^{14} Hz. At this frequency, the thickness of silicon nitride membrane is comparable to the wavelength, so it affects the transmission and reflection (1.2–4.2 μm). Figures 3(c) and (d) show that intrinsic absorption of the Si_3N_4 membrane in the NIR range is almost 0, while with the PyC coating it is at least 10% with some variation as a function of frequency. This absorption is less than the 40% value expected for a free-standing conductive PyC with frequency-independent conductivity.

More detailed analysis of the frequency dependence of the PyC absorptivity is based on the Drude–Lorentz model for PyC [31, 32] and Lorentz model for the Si_3N_4 membrane. That in the case of the conductive PyC film we approximate the dielectric function as:

$$\varepsilon_{\mathrm{PyC}}(\omega) = \varepsilon_\infty + A_\mathrm{T}\frac{\omega_\mathrm{T}}{\omega_\mathrm{T}^2 - \omega^2 - i\omega\gamma_\mathrm{T}} - \varepsilon_\infty\frac{4\pi\sigma_\mathrm{DC}}{i\omega(1 - i\omega\tau)} \tag{2}$$

and in the case of the bare Si_3N_4 membrane:

$$\varepsilon_{\mathrm{Si_3N_4}}(\omega) = \varepsilon_\infty + A_\mathrm{T}\frac{\omega_\mathrm{T}}{\omega_\mathrm{T}^2 - \omega^2 - i\omega\gamma_\mathrm{T}}. \tag{3}$$

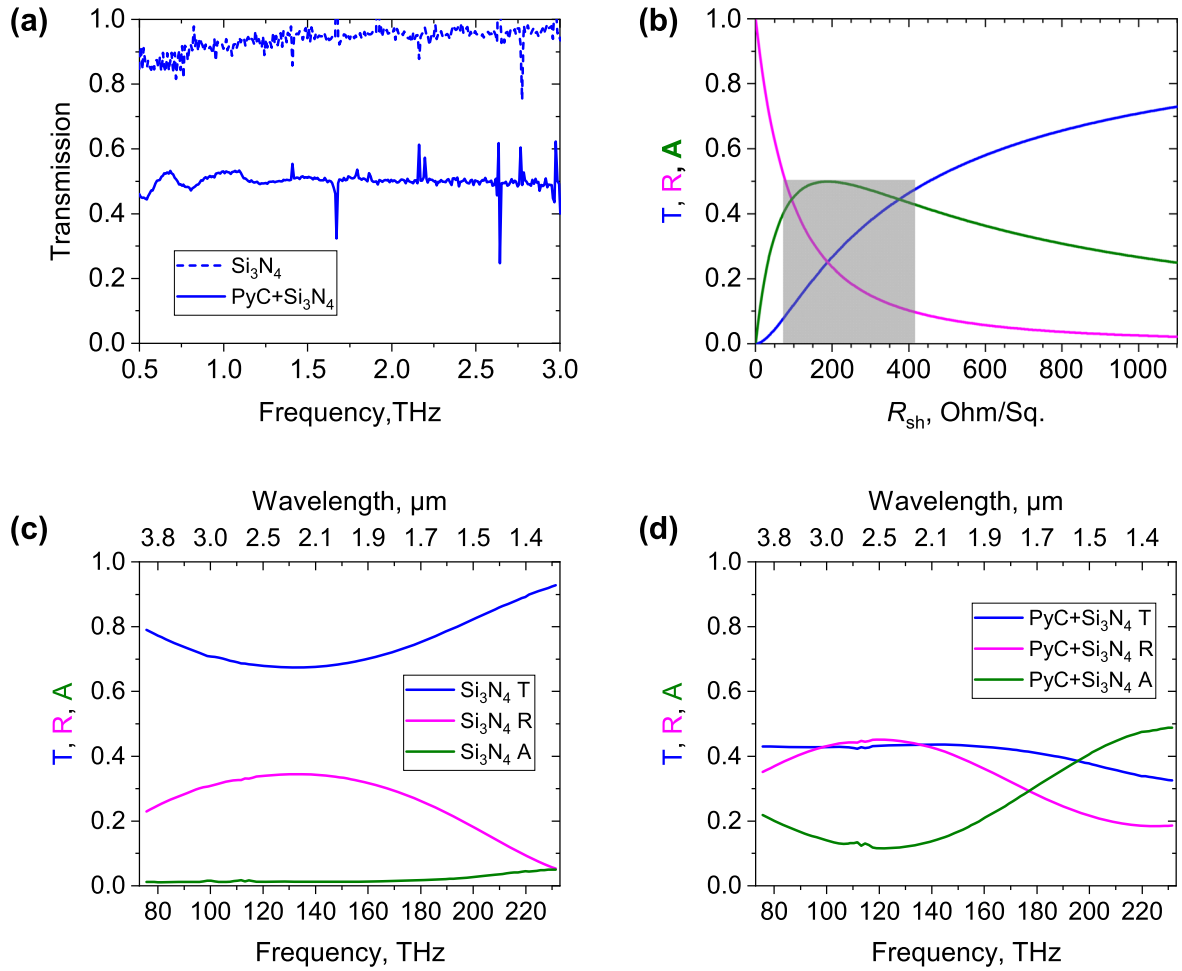

Figure 3. (a) Transmission of the bare 300 nm thick Si_3N_4 membrane (blue dashed line) and a PyC coated Si_3N_4 membrane (blue solid line) in the THz range. (b) Reflection (R), transmission (T), and absorption (A) of a thin conductive film as a function of its sheet resistance calculated based on the [18]. The shaded region marks the range of the film sheet resistance corresponding to more than 40% absorption. Reflection, transmission, and absorption of a Si_3N_4 membrane (c) and PyC coated Si_3N_4 membrane (d) measured in the NIR range.

Table 1. Material parameters used for spectra calculation.

	ε	ω_T, Hz	A_T	γ_T, Hz	σ_{DC}, S/m	τ, fs
Si_3N_4	3.85	1.6×10^{14}	3	2.4×10^{13}	—	—
PyC	1.2	7×10^{15}	4	8.5×10^{15}	8×10^{4}	2

The second term equation (2) describes the contribution of the π–π^* electron transitions ($E_T = \hbar\omega_T = 4.6$ eV) to the dielectric function. The transition strength A_T and the full width at half maximum (FWHM) γ_T, as well as the high frequency dielectric permittivity ε_∞, have been determined in earlier work [31]. The third term in equation (2) describes the contribution of the free charge carriers via Drude model with DC conductivity σ_{DC} and carrier scattering time τ. In the equation (3), the third term responsible for free carrier absorption is zero, while the second term describes the resonant absorption at $\omega_T \approx 1.6 \times 10^{14}$ Hz due to the optical phonon excitation (see [33, 34]). Note that, $\omega_T = 2\pi f_T$, where f_T is the frequency at which we see the absorption maximum around 26 THz.

The reflection, transmission, and absorption spectra of the bare Si_3N_4 membrane as well as the PyC coated one can be simulated by the standard transfer matrix method using the above formulae for the dielectric functions. The table 1 summarizes the values of parameters that provide best match between the simulated and measured spectra. The resultant calculated spectra and experimental data are shown in figures 4(a), (b).

Parameters for Si_3N_4 are consistent with those reported in [33] and [34]. Fitting parameters for the Lorentz term in equation (2) are taken from the [31] while the scattering time τ is consistent with an estimation $\tau \approx l/v_F$ with $l \sim 5$ nm being the average graphene flake size and $v_F \approx 10^6$ m s^{-1} is the Fermi velocity in the graphene.

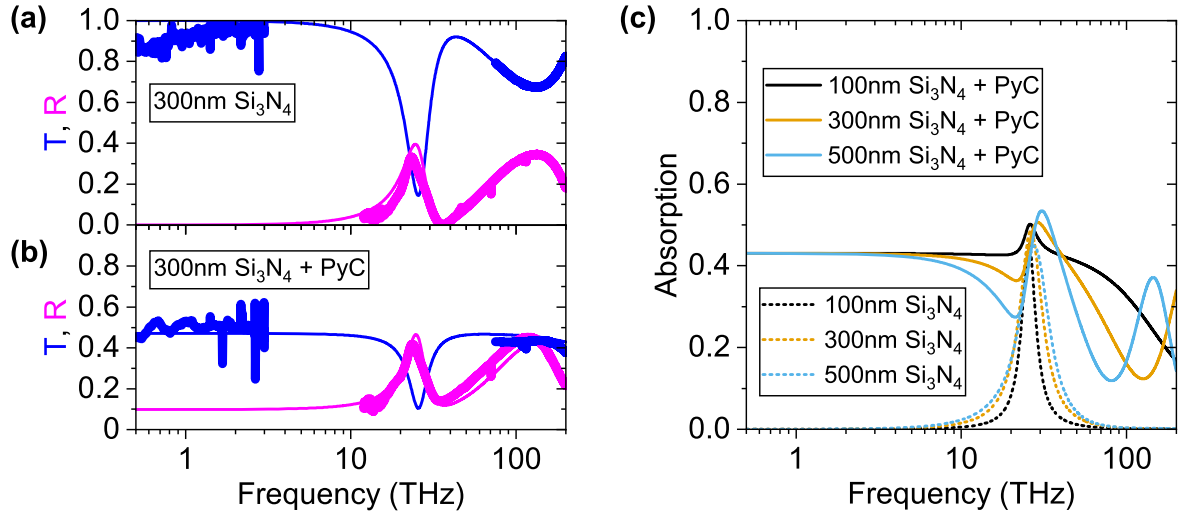

Figure 4. Effect of PyC coating on the optical properties of the Si_3N_4 membrane. (a) Calculated (lines) and measured (thick lines) transmission T (blue) and reflection R (magenta) spectra of a 300 nm Si_3N_4 membrane. (b) Same for a 300 nm Si_3N_4 membrane with a 20 nm PyC coating. (c) Calculated absorption of bare Si_3N_4 membrane and of Si_3N_4 membrane with a PyC coating at different Si_3N_4 thicknesses.

The good agreement between the calculated and the measured spectra gives confidence in predictions of the simulations in the entire frequency range from 0.5 to 200 THz and in particular the predicted absorption of the Si_3N_4-PyC as shown in in the figure 4(c). While radiation absorption by bare Si_3N_4 membrane is nonzero only around the optical phonon frequency, the PyC coated membrane is predicted to absorb regardless of the Si_3N_4 membrane thickness. Morphology and homogeneity of the PyC films at the interface with different substrates was studies in several earlier works [35–37]. Based on these results we conclude that local changes of the film conductivity at the interface with the membrane cannot cause significant change in the interaction with the electromagnetic radiation in a wide frequency range consistently with our results.

It clearly demonstrates very good performance of a 20 nm PyC film at all frequencies where the Si_3N_4 membrane is not absorptive itself and could be including micromechanical bolometers, where the thin graphitic film can be safely embedded without degrading the resonator quality [38, 39].

4. Conclusions

To summarize, we report on one of the first successful attempts to fabricate nm-thin graphitic film on the top of optically thin suspended dielectric membrane transparent in the ultrabroad spectral range spanning from THz to IR. The 300 nm thick Si_3N_4 membrane was covered with 20 nm thick pyrolytic carbon via chemical vapor deposition process. We have shown that a 20 nm thick PyC film placed on a Si_3N_4 membrane absorbs up to 40% of the incident THz radiation, close to the maximum amount possible for the planar thin conductive film, and no less 10% in NIR radiation. The results clearly demonstrates very good performance of a 20 nm PyC film at all frequencies where the Si_3N_4 membrane does not absorb and therefore it can be used with micromechanical bolometers. The fabrication of the PyC covered silicon nitride membrane relies on reproducible routines. The transport properties and morphology of the graphitic film remain intact after several fabrication steps including reactive ion etching of the silicon nitride and wet etching of silicon. Given the low density of the PyC film, our results open new opportunities for ultrabroad bolometers. Our experimental data along with a simple model describing the optical response of the PyC film facilitate designing THz/IR optoelectronic devices, based on the chemically robust and biocompatible PyC film.

Acknowledgments

The study was accomplished with the financial support of subproject H-Cube of EU ATTRACT phase 2 Research infrastructure H2020 (Project № 101004462), Academy of Finland (Flagship Programme PREIN, decision 320166 and 346518, prj. 343393), Horizon 2020 RISE DiSeTCom (Project № 823728), TERASSE Project (Project № 823878) and COST Action NanoSpace (Project № CA21126). The Vilnius Group acknowledges the Research Council of Lithuania for financial support through the 'T-HP' Project under Grant DOTSUT-184 funded by the European Regional Development Fund according to the supported activity 'Research Projects Implemented by World-Class Researcher Groups' under Contract 01.2.2-LMT-K-718-03-0096.

Data availability statement

All data that support the findings of this study are included within the article (and any supplementary files).

ORCID iDs

Justinas Jorudas https://orcid.org/0000-0001-5629-8545
Daniil Pashnev https://orcid.org/0000-0002-4648-0957
Andrzej Urbanowicz https://orcid.org/0000-0002-2769-452X
Irmantas Kašalynas https://orcid.org/0000-0003-1256-9424
Alessandro Pitanti https://orcid.org/0000-0002-7027-0300
Sergei Malykhin https://orcid.org/0000-0001-7677-0739
Polina Kuzhir https://orcid.org/0000-0003-3689-0837
Georgy Fedorov https://orcid.org/0000-0002-5224-0474

References

[1] Kuzhir P P, Paddubskaya A G, Volynets N I, Batrakov K G, Kaplas T, Lamberti P, Kotsilkova R and Lambin P 2017 Main Principles of passive devices based on graphene and carbon films in microwave—thz frequency range *J. Nanophotonics* **11** 032504
[2] Kuzhir P, Celzard A and Chen X 2022 Microwave absorption by carbon-based materials and structures *J. Appl. Phys.* **131** 200401
[3] Wang X-C, Diaz-Rubio A and Tretyakov S A 2017 An accurate method for measuring the sheet impedance of thin conductive films at microwave and millimeter-wave frequencies *IEEE Trans. Microw. Theory Tech.* **65** 5009–18
[4] Silva Z J, Valenta C R and Durgin G D 2021 Optically Transparent antennas: a survey of transparent microwave conductor performance and applications *IEEE Antennas Propag. Mag.* **63** 27–39
[5] Šlegerytė V, Belova-Plonienė D, Katkevičius A and Plonis D 2019 Microwave devices with graphene layers: a review. *In Proc. of the 2019 IEEE Microwave Theory and Techniques in Wireless Communications (MTTW) (Piscataway, NJ)* (IEEE) 87–92
[6] Wang L, Yu X, Li X, Zhang J, Wang M and Che R 2019 Conductive-network enhanced microwave absorption performance from carbon coated defect-Rich Fe_2O_3 anchored on multi-wall carbon nanotubes *Carbon* **155** 298–308
[7] Pang H *et al* 2021 Research advances in composition, structure and mechanisms of microwave absorbing materials *Composites* B **224** 109173
[8] Baah M *et al* 2021 All-graphene perfect broadband THz absorber *Carbon* **185** 709–16
[9] Novitsky A, Paddubskaya A, Otoo I A, Pekkarinen M, Svirko Y and Kuzhir P 2022 Random graphene metasurfaces: diffraction theory and giant broadband absorptivity *Phys. Rev. Appl.* **17** 044041
[10] Batrakov K, Kuzhir P, Maksimenko S, Paddubskaya A, Voronovich S, Kaplas T and Svirko Y 2013 Enhanced microwave shielding effectiveness of ultrathin pyrolytic carbon films *Appl. Phys. Lett.* **103** 073117
[11] Lee H, Paeng K and Kim I S 2018 A review of doping modulation in graphene *Synth. Met.* **244** 36–47
[12] Chen S *et al* 2021 Electrically tunable correlated and topological states in twisted monolayer–bilayer graphene *Nat. Phys.* **17** 374–80
[13] Tasolamprou A C *et al* 2019 Experimental demonstration of ultrafast THz modulation in a graphene-based thin film absorber through negative photoinduced conductivity *ACS Photonics* **6** 720–7
[14] Han M, Mu Y, Yuan F, Liang J, Jiang T, Bai X and Yu J 2020 Vertical graphene growth on uniformly dispersed sub-nanoscale SiO_x/N-doped carbon composite microspheres with a 3D conductive network and an ultra-low volume deformation for fast and stable lithium-Ion Storage *J. Mater. Chem.* A **8** 3822–33
[15] Sassi U *et al* 2017 Graphene-based mid-infrared room-temperature pyroelectric bolometers with ultrahigh temperature coefficient of resistance *Nat. Commun.* **8** 14311
[16] Lee G-H *et al* 2020 Graphene-based josephson junction microwave bolometer *Nature* **586** 42–6
[17] Liu Z, Liang Z, Tang W and Xu X 2020 Design and fabrication of low-deformation micro-bolometers for THz detectors *Infrared Phys. Technol.* **105** 103241
[18] Bosman H, Lau Y Y and Gilgenbach R M 2003 Microwave absorption on a thin film *Appl. Phys. Lett.* **82** 1353–5
[19] Ling C C, Landry J C, Davee H, Chin G and Rebeiz G M 1994 Large area bolometers for thz power measurements *IEEE Trans. Microw. Theory Tech.* **42** 758–60
[20] Antonets I V, Kotov L N, Nekipelov S V and Karpushov E N 2004 Conducting and reflecting properties of thin metal films *Tech. Phys.* **49** 1496–500
[21] Mahan G D and Marple D T F 1983 Infrared absorption of thin metal films: Pt on Si *Appl. Phys. Lett.* **42** 219–21
[22] Kašalynas I, Adam A J L, Klaassen T O, Hovenier J N, Pandraud G, Iordanov V P and Sarro P M 2008 Design and performance of a room-temperature terahertz detection array for real-time imaging *IEEE J. Sel. Top. Quantum Electron.* **14** 363–9
[23] McEvoy N, Peltekis N, Kumar S, Rezvani E, Nolan H, Keeley G P, Blau W J and Duesberg G S 2012 Synthesis and analysis of thin conducting pyrolytic carbon films *Carbon* **50** 1216–26
[24] Heikkinen J J, Košir J, Jokinen V and Franssila S 2020 Fabrication and design rules of three dimensional pyrolytic carbon suspended microstructures *J. Micromech. Microeng.* **30** 115003
[25] Kuzhir P P, Paddubskaya A G, Maksimenko S A, Kaplas T and Svirko Y 2013 Microwave absorption properties of pyrolytic carbon nanofilm *Nanoscale Res. Lett.* **8** 60
[26] Kotsilkova R, Todorov P, Ivanov E, Kaplas T, Svirko Y, Paddubskaya A and Kuzhir P 2016 Mechanical properties investigation of bilayer graphene/poly(methyl methacrylate) thin films at macro, micro and nanoscale *Carbon* **100** 355–66
[27] Benzinger W, Becker A and Hüttinger K J 1996 Chemistry and kinetics of chemical vapour deposition of pyrocarbon: I. fundamentals of kinetics and chemical reaction engineering *Carbon* **34** 957–66
[28] Nuss M C and Orenstein J Terahertz time-domain spectroscopy *In Millimeter and Submillimeter Wave Spectroscopy of Solids* (Springer) pp 7–50
[29] Gaffney J S, Marley N A and Jones D E 2012 Fourier transform infrared (FTIR) spectroscopy *In Characterization of Materials* (Wiley) pp 1–33
[30] Matthews M J, Pimenta M A, Dresselhaus G, Dresselhaus M S and Endo M 1999 Origin of dispersive effects of the raman D Band in carbon materials *Phys. Rev.* B **59** R6585–8
[31] Dovbeshko G I, Romanyuk V R, Pidgirnyi D V, Cherepanov V V, Andreev E O, Levin V M, Kuzhir P P, Kaplas T and Svirko Y P 2015 Optical properties of pyrolytic carbon films versus graphite and graphene *Nanoscale Res. Lett.* **10** 234
[32] Adamov R B *et al* 2021 Optical performance of two dimensional electron gas and gan: C buffer layers in AlGaN/AlN/GaN heterostructures on SiC substrate *Appl. Sci.* **11** 6053

[33] Wada N, Solin S A, Wong J and Prochazka S 1981 Raman and IR absorption spectroscopic studies on α, β, and amorphous Si3N4 *J. Non. Cryst. Solids* **43** 7–15
[34] Knolle W R and Allara D L 1986 Infrared spectroscopic characterization of silicon nitride films—optical dispersion induced frequency shifts *Appl. Spectrosc.* **40** 1046–9
[35] Baryshevsky V *et al* 2015 Study of nanometric thin pyrolytic carbon films for explosive electron emission cathode in high-voltage planar diode *Thin Solid Films* **581** 107–11
[36] Vogel W and Hosemann R 1979 The paracrystalline nature of pyrolytic carbons *Carbon* **17** 41–8
[37] Zhang X, Zhong L, Mateos A, Kudo A, Vyatskikh A, Gao H, Greer J R and Li X 2019 Theoretical strength and rubber-like behaviour in micro-sized pyrolytic carbon *Nat. Nanotechnol.* **14** 762–9
[38] Vicarelli L, Tredicucci A and Pitanti A 2022 Micromechanical bolometers for subterahertz detection at room temperature *ACS Photonics* **9** 360–7
[39] Piller M, Hiesberger J, Wistrela E, Martini P, Luhmann N and Schmid S 2023 Thermal IR detection with nanoelectromechanical silicon nitride trampoline resonators *IEEE Sens. J.* **23** 1066–71